J Biol Inorg Chem (2003) 8: 810–814
DOI 10.1007/s00775-003-0483-2

ORIGINAL ARTICLE

María J. Jurado · Vidal Barrón · José Torrent

Can the presence of structural phosphorus help to discriminate between abiogenic and biogenic magnetites?

Received: 3 March 2003 / Accepted: 7 July 2003 / Published online: 27 August 2003

Abstract The influence of phosphate on the competitive formation of magnetite and lepidocrocite and the properties of magnetite prepared from mixtures of Fe(II) and Fe(III) salts were studied. Products were prepared at 90 °C and pH 12.5 (series 1), 50 °C and pH 7 (series 2) and 20 °C and pH 8 (series 3). The P/Fe atomic ratio in the initial solution ranged from 0 to 3% and the pH was kept at the desired value with NaOH or KOH. Air was used as oxidant in series 2 and 3. All products, which were characterized by X-ray diffraction, transmission electron microscopy, chemical analysis and IR spectroscopy, contained a phase intermediate between magnetite and maghemite (referred to as magnetite in this paper). The products of series 1 consisted only of magnetite at all P/Fe ratios, whereas both magnetite and lepidocrocite formed in series 2 and 3 above a certain P/Fe ratio. On increasing the P/Fe ratio in the initial solution, the magnetite crystals became smaller and more oxidized (i.e. closer to maghemite) and the lepidocrocite/magnetite ratio increased. The P associated with magnetite was partly in the form of occluded P, i.e. non-surface-adsorbed phosphate. IR spectra suggested this P to be structural and occurring as low-symmetry PO_4 units. Because abiogenic magnetites produced in various environments incorporate structural P but some well-characterized biogenic magnetites seem to contain no P or be formed in P-poor environments, we hypothesize that natural magnetites containing occluded P are unlikely to be biogenic. However, more studies are needed to discard the presence of P in biogenic magnetites.

Keywords Lepidocrocite · Maghemite · Magnetite · Phosphorus/iron atomic ratio · Structural phosphorus

M. J. Jurado · V. Barrón · J. Torrent (✉)
Departamento de Ciencias y Recursos Agrícolas y Forestales,
Universidad de Córdoba,
Apdo. 3048, 14080 Córdoba, Spain
E-mail: torrent@uco.es
Tel.: +34-957-218472
Fax: +34-957-218440

Introduction

Foreign ions can control the transformation of iron salts and poorly crystalline Fe oxides into crystalline phases. In particular, phosphate, a ubiquitous anion in soils, sediments and other environments, strongly influences the nature and crystallochemical properties of the natural Fe oxides, hydroxides and oxyhydroxides (referred to as Fe oxides in this article) [1].

Laboratory experiments showed that ferrihydrite doped with phosphate transformed into poorly crystalline lepidocrocite, or did not undergo significant transformation when the P/Fe atomic ratio was > 2.5–3% [2]. However, for P/Fe atomic ratios of about 2.75%, ferrihydrite slowly transforms into maghemite, in what is possibly a simple pathway to maghemite in Earth and Mars soils [3]. Small amounts of phosphate favored the formation of hematite over goethite and influenced markedly the crystal morphology of these two oxides when ferrihydrite was the precursor [2]. Oxidation of Fe(II) salts precipitated with bicarbonate resulted in a mixture of goethite and lepidocrocite at $P/Fe < 0.01$, but only nanophase lepidocrocite at $0.01 < P/Fe < 0.2$ [4]. In some of these experiments, hematite and lepidocrocite (but not goethite) incorporated phosphorus in an occluded (i.e. non-surface-adsorbed) form.

Natural Fe oxides occur not only in the lithosphere and pedosphere, but also in the biosphere. Goethite, lepidocrocite, ferrihydrite and magnetite have been found in various living organisms, where they influence iron metabolism, are responsible for magnetotaxis, and provide support and hardness to biostructures such as teeth [5, 6]. In the case of magnetite, a debate is centered on the nature of the magnetic grains in the Martian ALH84001 meteorite, which, according to some authors, are fossil bacterial magnetosomes [7, 8], but, according to others, have an inorganic origin [9, 10]. Bacterial magnetosomes are made of idiomorphic magnetite grains enveloped by a membrane that prevents diffusion of phosphate, which mostly accumulates in

other intracellular granules containing poorly crystalline Fe oxides [11]. The formation of bacterial magnetite in an apparently phosphate-poor environment is possibly one of the factors contributing to the high chemical purity of magnetosomes [8]. Other biogenic magnetites seem also to occur in P-poor environments. For instance, the radula teeth of chitons (Mollusca) exhibit an external layer of magnetite that is not in direct contact with the calcium phosphate tooth nucleus but separated from it by a thin layer of lepidocrocite [12].

The objectives of this work were: (1) to study the effect of phosphate on the competitive formation of lepidocrocite and magnetite from a mixture of Fe(II) and Fe(III) salt solutions, and (2) to characterize the crystallochemical properties of the synthesized magnetites, paying special attention to the possible presence of P occluded in a structural form. It was hypothesized that such presence might be a useful criterion to differentiate between abiogenic (inorganic) and biogenic magnetites.

Materials and methods

Various series of black magnetic precipitates were obtained by treating mixtures of Fe(II) and Fe(III) salt solutions with varying concentrations of phosphate with NaOH or KOH and keeping pH constant with a pH-stat. To obtain magnetites exhibiting different properties, three series were prepared. Series 1 was prepared at 90 °C and pH 12.5, series 2 at 50 °C and pH 7, and series 3 at 20 °C and pH 8. Phosphate (0.1 M KH_2PO_4) was added to the initial solution, so that the range in the P/Fe atomic ratio was 0–3% in all series (P/Fe values higher than 3% were not used because magnetite crystallization is severely inhibited at such high ratios [13]). The magnetites of series 1 were prepared according to the method of Schwertmann and Cornell [14], which requires no oxidation, and the method of Taylor et al. [15], which requires oxidation with air, was followed for series 2 and 3. After synthesis, the suspension was centrifuged, the sediment washed several times with water, and the resulting suspension dialyzed in deionized water until the electrical conductivity of the equilibrium solution was <1 mS m^{-1}. Then, the suspension was freeze-dried and the solid products kept in stoppered polyethylene tubes.

Total Fe and P (Fe_t, P_t) and Fe(II) in the solid products were determined after dissolving 25 mg of the product in 1 mL of cold 11 M HCl. Then, Fe_t and Fe(II) in solution were determined by the *o*-phenanthroline method [16], except that no hydroxylamine was used in the determination of Fe(II). In both cases, absorbance was measured at 508 nm in a Perkin-Elmer Lambda 3 UV-visible spectrophotometer. Total P was determined by the molybdenum blue method [17], absorbance being measured at 712 nm with the spectrophotometer cited before. The NaOH-extractable P (P_{NaOH}) in the solid products was determined by shaking a 10-mg sample in 5 mL of 0.1 M NaOH at 25 °C for 16 h. To study the acid dissolution kinetics, 20 mg of the product were first washed with 0.1 M NaOH to remove surface-adsorbed phosphate, suspended in 2 mL of 8 M HCl/0.8 M H_2SO_4, and shaken in a reciprocating shaker set at 120 oscillations min^{-1}. Portions of the suspension were taken at times ranging from 5 to 360 min and immediately centrifuged to separate the supernatant, which was analyzed for P, Fe_t and Fe(II) by the methods cited before.

Powder X-ray diffraction (XRD) patterns were obtained with a Siemens D5000 diffractometer equipped with Co Kα radiation and a graphite monochromator at a step size of 0.02° for 2θ and a counting time of 10 s. Phase and crystal parameters were calculated by using the Rietveld refinement [18] with the GSAS computer program [19]. The mean coherence length (MCL) was calculated from the full width at half height (given by the Rietveld refinement) by using the Scherrer equation. Transmission electron micrographs (TEM) were obtained with a Jeol-200 CX electron microscope. The specific surface area was determined by N_2 adsorption using the BET method in a Micromeritics ASAP 2010 surface area analyzer. IR spectra of KBr pellets (0.5 wt% sample) were recorded from 380 to 4000 cm^{-1} with a Perkin-Elmer 2000 FTIR spectrometer using 4 cm^{-1} resolution and an average of 64 scans.

Results and discussion

Nature of the synthesized products

The most relevant crystal properties of the products synthesized in the three series and the XRD patterns are shown in Table 1 and Fig. 1, respectively. The products contained or consisted exclusively of a magnetic phase intermediate between magnetite and maghemite (subsequently referred to as magnetite in this paper). It must be remembered here that these two isostructural minerals possess an inverse spinel structure [in magnetite, the unit cell contains 32 O and 24 Fe sites, with 8 Fe(II) in octahedral sites, 8 Fe(III) in octahedral sites and 8 Fe(III) in tetrahedral sites; in maghemite, little Fe(II) is present and the O:Fe ratio is 1.33 to 1.5]. Poorly crystalline lepidocrocite was formed, in addition to magnetite, at P/Fe > 2% (series 2) or > 1% (series 3). The Fe(II)/Fe_t ratio of magnetite (Table 1) was substantially lower than that of stoichiometric magnetite (0.33) and decreased with increasing P/Fe in the initial solution. The decrease in Fe(II)/Fe_t was concomitant with a

Table 1 Properties of the products

Temperature, pH during the synthesis	P/Fe[a] (%)	Mineralogical composition[b]	MCL[c] of magnetite[b] (nm)	Specific surface area (m^2 g^{-1})	Fe(II)/Fe_t(%)
90 °C, pH 12.5	0	MT	43	17	22.1
	1	MT	36	21	21.6
	2	MT	25	33	16.6
	3	MT	24	31	15.0
50 °C, pH 7	0	MT	21	75	11.5
	1	MT	26	29	13.1
	2	MT	20	86	10.2
	3	LP + MT	9	–	4.5
20 °C, pH 8	0	MT	17	95	10.1
	1	MT	22	62	9.1
	2	LP + MT	10	–	3.5
	3	LP + MT	2	–	3.7

[a]Atomic ratio
[b]MT = magnetite (the term used here to designate a magnetite–maghemite intermediate; LP = lepidocrocite
[c]MCL = mean coherence length

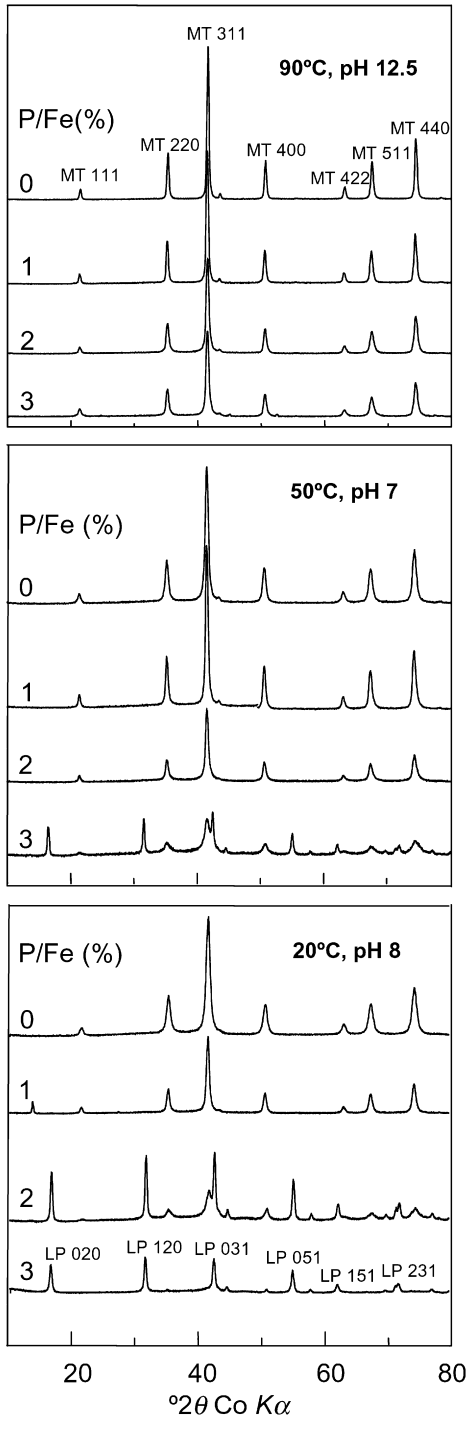

Fig. 1 X-ray diffraction patterns of the products synthesized at different temperature and pH values as a function of the P/Fe atomic ratio of the initial solution. The most characteristic magnetite–maghemite (MT) and lepidocrocite (LP) reflections are labeled

decrease in the *a* unit-cell edge length (Fig. 2), the reason being that *a* is slightly smaller in maghemite than in magnetite (0.834 versus 0.839 nm) [1]. We calculated the specific surface area (SSA) of magnetite in the lepidocrocite-free samples on the assumption that the crystals were cubes with a specific gravity of 5 and size equal to MCL. The SSA calculated in this way (detailed values not shown) was 40–60% higher than the measured (BET) SSA for the samples with $Fe(II)/Fe_t > 12\%$, which suggests some degree of multidomainicity in these samples. The opposite was true for the samples with $Fe(II)/Fe_t < 12\%$, which suggests greater surface rugosity and presence of mesopores (no micropores were present according to the t-plot method) in these more oxidized magnetites.

In the products that contained lepidocrocite, the lepidocrocite/magnetite ratio increased with increasing P/Fe (Table 1; Figs. 1 and 3). Mann et al. [20] synthesized magnetite in the presence of phosphate via green rust but did not find lepidocrocite as either a final or an intermediate product, probably because the P/Fe range in which lepidocrocite forms is narrow. However, it must be remembered that, for suitable P/Fe values, lepidocrocite is readily formed from different precursors including P-doped ferrihydrites [2] and Fe(II) salts precipitated with bicarbonate and oxidized with air [4]. Also, in vitro oxidation at room temperature of vivianite [$Fe_3(PO_4)_2 \cdot 8H_2O$, a mineral found in reductive environments and used as a slow-release P and Fe fertilizer] results in the formation of poorly crystalline lepidocrocite [21]. In summary, lepidocrocite, rather than other Fe oxides, is formed and/or persists in chemical environments where phosphate is present in significant concentration. The "pro-lepidocrocite" effect of phosphate observed in laboratory experiments appears to be consistent with the above-mentioned observation that the calcium phosphate (apatite) core of the major lateral tooth of some chitons of genus *Acanthopleura* is separated from the magnetite in the posterior region of the tooth cusp by a layer of lepidocrocite [12, 22]. It can be speculated that the high concentration of P in solution that probably precedes apatite precipitation favors lepidocrocite over magnetite in the latter stages of iron mineralization in the tooth core region.

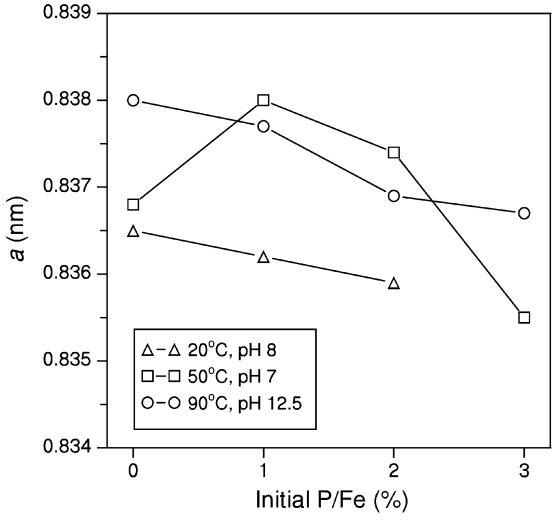

Fig. 2 The unit-cell edge length, *a*, for the magnetite–maghemite phase as a function of the P/Fe atomic ratio of the initial solution

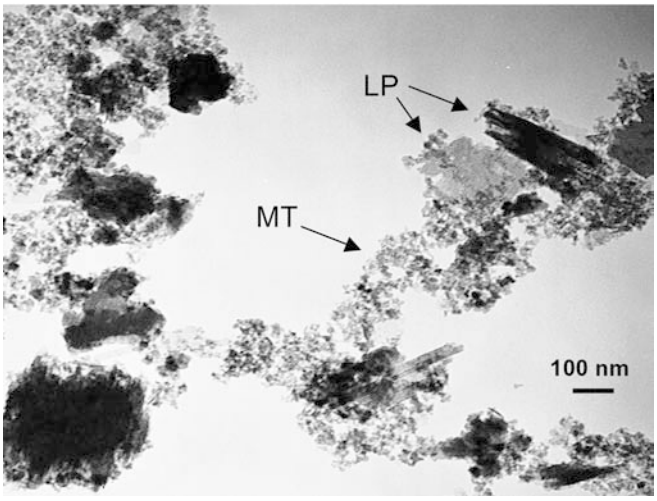

Fig. 3 Transmission electron micrograph of the sample synthesized at 20 °C, pH 8 and 2% P/Fe ratio of the initial solution. According to the selected area electron diffraction patterns, the pseudohexagonal and subrounded particles are magnetite–maghemite (MT) and the platy particles partially surrounded by the former are lepidocrocite (LP)

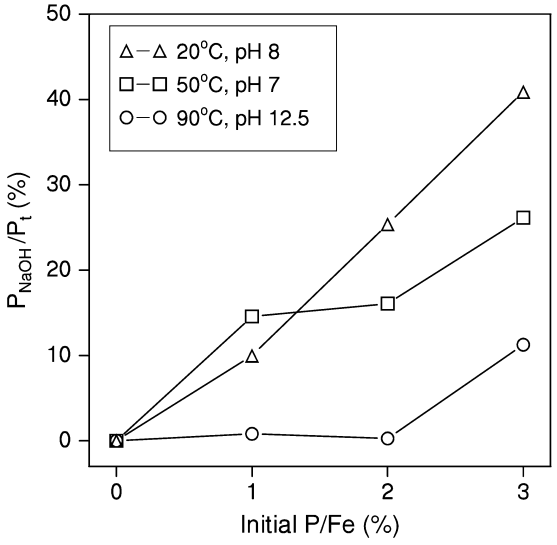

Fig. 4 The ratio of NaOH-extractable P to total P (P_{NaOH}/P_t) in the solid products as a function of the P/Fe ratio of the initial solution

Forms of phosphate in the products

After synthesis, >99% of the P remained associated with the solid products (i.e. the Fe oxides) except for the samples prepared at 90 °C and pH 12.5 and P/Fe > 1%, where this proportion was >75%. The NaOH-extractable P of the solid products, which is generally considered as the surface adsorbed phosphate [23], was in all cases less than 40% of total P (Fig. 4). The products synthesized at low temperatures and/or a higher initial P/Fe ratio exhibited higher P_{NaOH}/P_t ratios than the other products, probably because (1) their particles were small and hence the surface/bulk ratio large, and (2) some products contained poorly crystalline lepidocrocite and, possibly, traces of ferrihydrite, which have a high phosphate sorption capacity [4]. In the products with only magnetite, P_{NaOH}/P_t was <20%. Consequently, magnetite was, under certain conditions, efficient to retain significant amounts of phosphate in a non-desorbable, occluded form.

Figure 5 shows the results of the acid dissolution experiments for selected samples plotted as percent dissolved P against percent dissolved Fe. The cubic curves that were used to fit and better visualize the data are close to the 1:1 line. This indicates that P and Fe tend to dissolve congruently, which is consistent with the idea that most P is homogeneously distributed in the magnetite crystals. The hypothesis that such P was structural could not be tested by examination of the P-induced changes in the *a* unit-cell edge length, the reason being that P indirectly affects *a* through its influence on the degree of oxidation of magnetite. Such a hypothesis, however, was supported by the IR spectra of the samples, as, for instance, the ones synthesized at 50 °C and pH 7 (Fig. 6). These spectra exhibit four distinctive

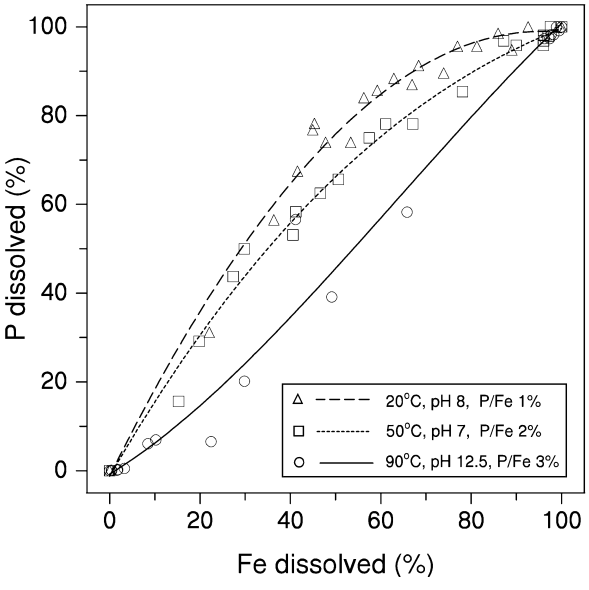

Fig. 5 Percent P against percent Fe that is dissolved in HCl/H_2SO_4 for three selected samples

bands in the P–O(H) stretching region at ~950, ~980, ~1020 and ~1080 cm^{-1}, the intensities of which increase with increasing P content. These bands: (1) differ from those due to phosphate adsorbed on P-free magnetite, which are quite broad and are seen at ~1040 and ~1130 cm^{-1} (spectra not shown), and (2) are close to those assigned to structural P present as low-symmetry PO_4 units in hematites prepared in the presence of P [24, 25], which supports the idea that P can be structurally accommodated in magnetite also.

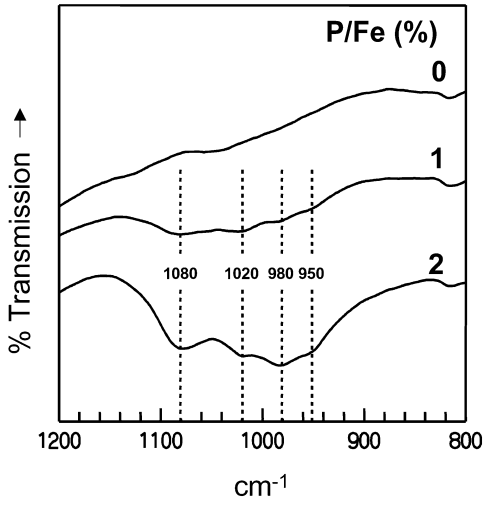

Fig. 6 Infrared spectra of the samples synthesized at 50 °C and pH 7 as a function of the P/Fe ratio of the initial solution

Structural P in relation to the origin of magnetite

The experiments reported here suggest that abiogenic magnetite is capable of incorporating P in structural form if synthesized in the presence of a medium containing phosphate. Such incorporation took place at temperatures and pH values similar to those of different hydrothermal and weathering environments. For instance, temperatures of ca. 20 °C and pH values in the vicinity of 8 occur in soils, where the inorganic formation of magnetite has been advocated [26]. By contrast, biogenic magnetites that have been studied in detail are rather pure [8, 27]. Moreover, current data on the genesis and distribution of the Fe oxides present in biota (e.g. in the teeth of chitons) indicate, as discussed before, that magnetite seems to occur and/or form in environments poor or depleted in P. Indeed, the need exists to systematically study biogenic magnetites of various origins (e.g. excretory granules in invertebrate species) to substantiate the hypothesis that biogenic magnetites do not contain structural P.

Acknowledgements This work was supported by the Spanish Ministry of Science and Technology (project PB98-1015). The authors wish to thank Profs. M.A. Aramendía and F. Urbano and Dr. A. Marinas, Departamento de Química Orgánica, Universidad de Córdoba, for their assistance with the IR analyses.

References

1. Cornell RM, Schwertmann U (1996) The iron oxides. VCH, Weinheim
2. Gálvez N, Barrón V, Torrent J (1999) Clays Clay Miner 47:304–311
3. Barrón V, Torrent J (2002) Geochim Cosmochim Acta 66:2801–2806
4. Cumplido J, Barrón V, Torrent J (2000) Clays Clay Miner 48:503–510
5. Lowenstam HA (1981) Science 211:1126–1131
6. Webb J, Macey DJ, Chua-anusorn W, St Pierre TG, Brooker LR, Rahman I, Noller B (1999) Coord Chem Rev 192:1199–1215
7. McKay DS, Gibson EK Jr, Thomas-Keprta KL, Vali H, Romanek CS, Clemett SJ, Chillier XD, Maechlingand CR, Zare RN (1996) Science 273:924–930
8. Thomas-Keprta KL, Bazylinski DA, Kirschvink JL, Clemett SJ, McKay DS, Wentworth SJ, Vali H, Everett KG Jr, Romanek CS (2000) Geochim Cosmochim Acta 64:4049–4081
9. Golden DC, Ming DW, Schwandt CS, Lauer HV Jr, Socki RA, Morris RV, Lofgren GE, McKay GA (2001) Am Miner 86:370–375
10. Barber DJ, Scott ERD (2002) Proc Natl Acad Sci USA 99:6556–6561
11. Lins U, Farina M (1999) FEMS Microbiol Lett 172:23–28
12. Lee P, Webb J, Macey DJ, van Bronswijk W, Savarese AR, de Witt GC (1998) J Biol Inorg Chem 3:614–619
13. Couling SB, Mann S (1985) J Chem Soc Chem Commun 1713–1715
14. Schwertmann U, Cornell RM (2000) Iron oxides in the laboratory: preparation and characterization. Wiley-VCH, Weinheim
15. Taylor RM, Maher BA, Self PG (1987) Clay Miner 22:411–422
16. Olson RV, Ellis R Jr (1982) In: Page AL, Miller RH, Keeney DR (eds) Methods of soil analysis, part 2. ASA and SSSA, Madison, Wisconsin, pp 310–312
17. Murphy J, Riley JA (1962) Anal Chim Acta 27:31–36
18. Rietveld HM (1967) Acta Crystallogr 22:151–152
19. Larson AC, Von Dreele RB (1988) GSAS: general structure analysis system. Los Alamos National Laboratory, Los Alamos, New Mexico
20. Mann S, Sparks HC, Couling SB, Larcombe MC, Frankel RB (1989) J Chem Soc Faraday Trans I 85:3033–3044
21. Roldán R, Barrón V, Torrent J (2002) Clay Miner 37:709–718
22. Lee P, Brooker LR, Macey DJ, van Bronswijk W, Webb J (2000) Calcif Tissue Int 67:408–415
23. Torrent J, Barrón V, Schwertmann U (1990) Soil Sci Soc Am J 54:1007–1012
24. Gálvez N, Barrón V, Torrent J (1999) Clays Clay Miner 47:375–385
25. Stachen M, Morales MP, Ocaña M, Serna CJ (1999) Phys Chem Chem Phys 1:4465–4471
26. Maher BA, Taylor RM (1988) Nature 336:368–370
27. Kirschvink JL, Kobayashi-Kirschvink A, Woodford BJ (1992) Proc Natl Acad Sci USA 89:7683–7687